Journal of Civil Engineering and Construction 2025;14(1):8-19
https://doi.org/10.32732/jcec.2025.14.1.8

A Microstructural Insight into the Hygrothermal Behaviour of Unstabilised and Cement Stabilised Compressed Earthen Bricks Exposed to High Temperatures

Rafik Abdallah[1], Agostino Walter Bruno[2], Céline Perlot[1,3], Hélène Carré[1]

1. Laboratoire SIAME, Fédération IPRA, EA4581, Université de Pau et des Pays de l'Adour, Anglet, France
2. Dipartimento di Ingegneria Civile, Chimica e Ambientale, Università degli studi di Genova, Genoa, Italy
3. Institut Universitaire de France, Paris, France
E-mail : rafik.abdallah@univ-pau.fr

Received: 11 December 2024; Accepted: 13 January 2025; Available online: 1 February 2025

Abstract: Earthen materials has received a lot of attention as a sustainable building material over the past few decades because of its eco-friendliness. As consequence of this renewed interest, numerous works have been recently developed on earthen materials, mostly with a focus on their mechanical behaviour. Conversely, there is still a significant gap in the literature on the understanding of the fire behaviour of earthen materials. Only a handful of studies has dealt with this subject and a systematic analysis on the causes of thermal instabilities in earth materials at high temperatures is still missing from the literature. The role played by the mineralogy of the earth materials on these thermal instabilities is still poorly understood and it requires further investigation. To fill these gaps, the present study presents the results from both mineralogical and hygrothermal tests performed on earth samples, which were either left unstabilised and compacted at 50 MPa or stabilised with cement and compacted at the optimum standard Proctor. Interestingly, unstabilised earthen samples exhibited thermal instabilities when exposed to high temperatures. To investigate deeper into the mineralogical causes of such thermal instabilities, samples were either equalised at the ambient temperature of about 25 °C or exposed at the high temperature of 350 °C before being subjected to thermogravimetric and differential scanning calorimetry (TG-DSC) tests, Fourier Transform Infrared (FTIR) spectroscopy tests, isothermal adsorption-desorption tests, and nitrogen gas permeability tests. Results show that cement stabilisation induced the formation of fresh the calcium-silicate-hydrate (C-S-H) and calcium-aluminate-hydrate (C-A-H) gels while reducing the water adsorption capacity. Both effects have rendered the material less prone to thermal instabilities compared to the unstabilised material. The main mineralogical and moisture-related changes influencing thermal and fire behavior might not be well captured by traditional studies. Though lacking in information to perform a thorough study, they do provide initial indications of possible internal alterations within the materials.
Keywords: Earthen materials; High temperature behaviour; Thermal instability; Earth mineralogy; Hygrothermal behaviour.

1. Introduction

The construction industry is undergoing a remarkable transformation with paradigm shifts involving both building practices and materials. In this context, earthen construction, which was traditionally overshadowed by fired earth, concrete, and other energy-intensive building materials, is now emerging as a promising alternative. Civil engineers, architects and building stakeholders are progressively rediscovering the green credentials of earthen materials, which could be a game-changing breakthrough in the construction industry. With a growing emphasis on sustainability and environmental awareness, earthen materials are gaining popularity for their unique combination of eco-friendliness, affordability, and versatility. Indeed, these materials possess an excellent ability to improve indoor comfort and building energy efficiency [1–3] combined with suitable hygro-thermo-mechanical characteristics [4–10].

However, the fire behaviour of these earthen materials is still poorly documented in the existing literature. Only a few studies have looked into this critical aspect, and the scarcity of available data makes it difficult to assess the reliability of earthen materials in fire-prone environments, particularly when it comes to the safety and well-being of residents. Recent work has been performed by Abdallah et al. (2024) [11–13], who studied the effect of compaction level water content and cement stabilisation on the fire behaviour of compressed earth bricks. Results showed that unstabilised earthen bricks, compacted at a high compaction pressure, exhibited thermal instabilities

(i.e. spalling, cracking, plastic deformation, detachment of heated fragments of surface layers) when exposed to ISO standard fire [14] after equalisation to intermediate water contents ranging between 3.2-5.7% corresponding to relative humidity levels of 50% and 75%. On the contrary, cement stabilisation prevented thermal instabilities under the same testing conditions. Results also highlighted that a coupled thermo-hydro-mechanical behaviour [11] may have played a critical role in the fire resistance of earthen materials. The second study [12] explored the impact of varying compaction pressures (5, 15, 30, and 50 MPa) on the thermal stability of CEBs under fire exposure. Bricks compacted at lower pressures (5 MPa) maintained stability, while those formed at higher pressures (15–50 MPa) experienced thermal instabilities, likely due to greater pore pressure accumulation and decreased permeability. Both investigations suggested that the fire response of earthen materials is influenced by thermo-hydro-mechanical interactions. These preliminary findings have opened up a fundamental research path towards the study of the fire behaviour of earthen building materials, which will be essential in both the patenting of these materials and their adoption into the construction mainstream.

To this end, this paper presents an in-depth examination of the influence of high temperature on the mineralogy and hygrothermal behaviour of both unstabilised and cement stabilised earth materials to further investigate the role of the previously mentioned thermo-hydro-mechanical coupling in the overall fire behaviour [11–13].

The approach adopted in this study consists of linking the thermo-hydro-mechanical coupling and the resulting fire behaviour of earth materials [11–13] with the changes in the mineralogical composition of the material after exposure to high temperatures. Some research works have already investigated the effects of fire and firing temperature on the microstructural properties of both unfired and fired soils under dry conditions [15–19]. However, to the best of the author's knowledge, no research has yet explored the connection between the fire resistance of earth materials and their coupled thermo-hydro-mechanical behavior concerning mineralogical changes in the context of earth-building construction. These internal thermal changes could have an impact, or not, on how earthen materials behave in a fire and may even be a factor in their thermal instability when exposed to fire.

Hence, this work presents results from an experimental campaign that investigates the effect of high-temperature exposure on the mineralogy and hygrothermal behaviour of both unstabilised and cement-stabilised earth materials. Thermogravimetric analyses, infrared spectroscopy tests, isothermal sorption-desorption tests, and residual nitrogen axial gas permeability tests were performed on both unstabilised and cement stabilised earth samples, which were either equalised at room temperature of 25 °C (i.e. benchmark), or exposed to the two temperatures of 80 °C (only for permeability tests) and 350 °C (for all tests). The latter temperature was chosen because it corresponds to the onset of thermal instabilities in compressed earthen bricks exposed to fire in which bricks started breaking and having a surface peeling [11]. Findings from the present experimental campaign will be discussed and linked to previous results in the literature regarding the high temperature/fire behaviour of earth materials.

2. Materials and methods

2.1 Raw materials

2.1.1 Soil

The soil used in the present experimental campaign was provided by the brickwork factory Nagen (Toulouse, France) and it is commonly used for manufacturing traditionnal fired bricks. Both the physical and compaction properties of the Nagen soil were measured by Bruno (2016) [20] and Bruno et al. (2019) [21], as summarised in Table 1. Additionally, Table 2 demonstrates the chemical composition of Nagen soil. Results show that the Nagen soil is a sandy silt with an illitic clay fraction of medium plasticity and an optimum standard Proctor water content of 12.5%, corresponding to a maximum dry density of 1948 kg/m^3.

Table 1. Physical and compaction characteristics of the soil used

Grain size distribution	
Clay (<0.002 mm)	16.3%
Silt (0.002-0.063 mm)	42.9%
Sand (0.063-2 mm)	40.4%
Gravel (>2 mm)	0.4%

Plasticity properties and activity	
Liquid limit, w_L	33.0%
Plastic limit, w_P	20.1%
Plasticity index, I_P	12.9%
Activity index, A	0.79

Standard Proctor compaction	
Optimum water content	12.5%
Maximum dry density	1948 kg.m^{-3}

Table 2. Chemical composition of the used soil

Chemical elements	SiO_2	AL_2O_3	MnO	MgO	CaO	Na_2O	K_2O	TiO_2	Fe_2O_3	P_2O_5
Percentage of oxides	54.60 %	16.30 %	0.056 %	2.64 %	4.77 %	0.59 %	2.88 %	0.70 %	5.80 %	0.14 %

2.1.2 Cement

Cement stabilised earth samples were manufactured by mixing the Nagen soil with CEM III /A 52.5 L CE, which is a cement blended with 61% by mass of blast furnace slag. This cement, purchased from EQIOM Group (Héming-France) and manufactured byfollowing the norm NF EN 197-1 (2012) [22], was selected because of its widespread availability and low clinker content (35%), which limits the environmental impact of the stabilisation.

2.2 Sample preparation

2.2.1 Selection of mixes

Two different material formulations were tested in the current work, namely unstabilised earth samples statically compacted at 50 MPa (named hereafter SW50) and earth samples compacted at the standard Proctor energy level and stabilised with 3.5% by soil dry mass of cement (named hereafter SWC3.5). These manufacturing methods and formulations were selected so that both SW50 and SWC3.5 samples exhibited an unconfined peak compressive strength of about 5 MPa after a previous equilibrium condition of 75 % RH [23], which is similar to that of standard hollow fired bricks [24].

2.2.2 Mixing

The soil was firstly dried for at least three days at a constant temperature of 80 °C, while mass measurements were taken every 24 hours until the mass difference was lower than 0.1% between two consecutive measurements. Then, SW50 samples were manufactured by mixing the dry soil with an optimum water content of 6.23% (percentage of dry soil weight) for a compaction effort of 50 MPa, as measured by Bruno (2016) [20] on the same soil. The moist soil was mixed for 10 minutes employing an electric planetary mixer to ensure good homogeneity of the water throughout the material mix.

SWC3.5 samples were instead mixed with a water content of 12.5% (percentage of dry soil weight), which corresponds to the optimum Proctor water content, plus additional water corresponding to 30% of the cement mass to ensure the complete hydration of the cement. A homogeneous cement paste was first formed by mixing the required water content and cement for 5 minutes and then mixed with the dry soil for 10 minutes with an electric planetary mixer.

2.2.3 Samples manufacturing

After mixing, the moist mixes were compacted in a hollow cylindrical mould to achieve a height of 50 mm and a diameter of 110 mm (Figure 1) for the subsequent permeability tests. Cylindrical samples were statically compacted, under displacement control, in three layers, each consisting of one-third of the entire sample mass. Each layer was compacted either to the target maximum dry density of 2223 kg/m^3 for SW50 samples [20], or to the target Proctor maximum dry density of 1948 kg/m^3 for SWC3.5 samples. This ensured an almost uniform density distribution across the entire specimen while scarification between the layers before compaction guaranteed proper layer bonding.

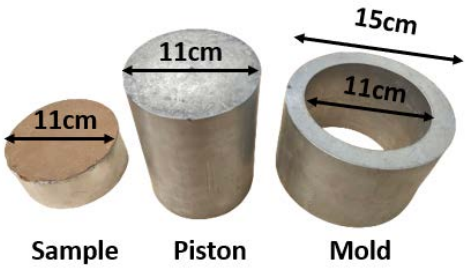

Figure 1. Cylindrical samples of 110 mm x 50 mm for permeability tests and compaction mould

2.2.4 Curing and equalisation

After compaction, cylindrical samples were sealed in plastic bags for 28 days to ensure an even distribution of water throughout the samples. Additionally, this curing phase also allowed for proper cement hydration in stabilised samples. To avoid any inaccurate influence on the samples' high temperature behaviour caused by

variable hygroscopic conditions [11–13], cylindrical samples were subsequently subjected to an equalisation phase to control the water content within the material. To this end, samples were placed in a tightly sealed container with a saturated sodium chloride solution, maintaining a relative humidity of 75% and a temperature range between 23 and 25 °C, for a minimum period of 14 days. This timeframe was sufficient to achieve equilibrium with sample mass variations lower than 0.1% over at least 24 hours. Note that the relative humidity level of 75% was selected because it corresponds to the upper limit of humidity range for indoor comfort [8], while also representing a particularly unfavourable condition for the onset of thermal instabilities for these materials, as experimentally shown by a previous study [11,12].

2.3 Exposure to high temperature

After equalisation, cylindrical samples were exposed to the two temperature levels, 80 and 350 °C, before characterisation. The temperature of 80 °C was selected to ensure the evaporation of bulk water without affecting the mineralogical phases and with only minimal changes in the material porosity [25]. The temperature of 350 °C was chosen because it corresponds to the onset of thermal instabilities within the earth materials, as detected by previous works in the literature [11,12]. Also, the burning out of the carbonaceous matter within the clay fraction starts approximately at 350 °C [26], which causes the mineral fabric to collapse into an illite-like structure [27].

Residual permeability tests required that the same specimen is initially exposed to 80 °C and subjected to a first round of permeability tests after being cooled down before being heated at 350 °C and then tested again after cooling. Drying at 80 °C was achieved through placing samples in an oven at 80 °C for enough time to cause sample masses to vary by less than 0.1% over the course of 24 hours. Further, this drying stage at 80 °C was needed to avoid that the presence of pore water could affect the permeability measurements, thus also resulting in a more complex analysis of permeability results.

Other cylindrical samples were either left at a room temperature of about 25 °C (i.e. control samples) or heated at a temperature of 350 °C before being subjected to thermogravimetric analyses, Fourier transform infrared spectroscopy, isothermal sorption-desorption and permeability tests.

Both SW50 and SWC3.5 samples were exposed to high temperatures inside an electric programmed oven, where the temperature was increased at a relatively low heating rate of 2 °C.min^{-1} up to its target value of 350 °C and then maintained constant for at least two hours. Afterwards, samples were cooled down to room temperature inside the oven at a rate of -2 °C.min^{-1}. The relatively low heating and cooling rate was chosen to limit the likelihood of thermal stresses within the samples, allowing for an improved evolution of material properties with temperature. The 2-hour plateau at constant temperature was needed to ensure a uniform temperature distribution throughout each sample. After cooling, the samples were stored in sealed containers containing silica gel until the day of testing. Further samples were subjected to laboratory tests (thermogravimetric and differential scanning calorimetry (TG-DSC), Fourier Transform Infrared (FTIR) spectroscopy, isothermal adsorption-desorption and nitrogen gas permeability), as it will be detailed in the following sections.

2.4 Testing methods

2.4.1 Thermogravimetric and differential scanning calorimetry (TG-DSC)

Both SW50 and SWC3.5 earthen samples, either equalised at 25 °C or heated at 350 °C, were subjected to Thermogravimetric-differential scanning calorimetry (TG-DSC) analyses to assess both the material stability and its composition/decomposition kinetics under varying temperature. TG-DSC analyses were carried out in an atmosphere of flowing oxygen-free N2 (40 cm3.min-1), in a Netzsch STA 449C TG-DSC system. During the analysis, an initial mass of about 50 mg of finely ground material was subjected to an increase of temperature up to 1000 °C with a constant rate of 10 °C.min-1. The mass loss during testing was measured with a balance with a resolution of 0.1 μg over the entire measuring range comprised between 0 and 35000 mg. The choice of performing TG-DSC tests on finely ground earth materials was dictated by the need of avoiding spurious gradient of temperature that could have occurred if compacted sample fragments were used instead. Results from TG-DSC tests are presented in the following section in terms of both mass loss and its derivative respect to the variation of temperature.

2.4.2 Fourier Transform Infra-Red (FTIR) spectroscopy

Fourier Transform Infrared (FTIR) spectroscopy tests were performed to analyse the effect of cement stabilisation and exposure to high temperatures on the nature of chemical bonds formed within the crystalline structure of both SW50 and SWC3.5 earth samples exposed either to 25 °C or to 350 °C. Before FTIR tests, the samples were uniformly and finely ground to avoid that coarse soil particles would trap infrared light beams, thus affecting transmittance measurements [28]. The fine powder was then dried inside sealed plastic boxes filled with silica gel at room temperature of 25 °C for a minimum period of 48 hours to limit the effect of pore water on the measured spectra. After drying, all samples were exposed to infrared light beams with a wavenumber ranging from

400 cm^{-1} to 4000 cm^{-1} while measurements of transmittance were simultaneously taken with a frequency of 1 cm^{-1}.

2.4.3 Isothermal sorption-desorption measure

Isothermal sorption- desorption curves were measured on both SW50 and SWC3.5 earth samples, which were preliminary exposed to either 25 °C or to 350 °C by means of the Dynamic Vapour Sorption (DVS) device commercialised by Surface Measurement Systems. Specimens of about 0.50 gram were primarily equalised at a relative humidity of 0% and at a constant temperature of 25 °C. DVS tests were then performed by placing each specimen on a plate connected to a balance with a resolution of 0.1 µg and inside a sealed chamber under controlled conditions of both temperature and relative humidity. The specimens were subjected to a stepwise increase of relative humidity up to 90% with successive 10% steps, plus a final stage at 95%, which is the maximum humidity that can be applied by the DVS device. Following the same stages of the adsorption branch, the relative humidity was subsequently decreased back to 0%, at a constant temperature of 25 °C. The sample mass was continuously recorded during the cyclic variation of relative humidity. Each stage lasted until the sample mass varied by less than 0.001% over a minimum time of 1 hour.

2.4.4 Nitrogen gas permeability tests

Nitrogen gas permeability tests were performed on cylindrical samples (11 cm diameter, 5 cm height) previously dried to allow the gas to fully enter the poral network for accurate characterisation it. Hence, samples equalised at room temperature were not subjected to permeability tests. The nitrogen gas permeability was measured by using a constant pressure permeameter designed according to the Cembureau guidelines [29]. Nitrogen gas was injected at different pressure levels (P_{inj}, Pa) ranging from 50000 to 150000 Pa, while the volumetric flow rate (Qv, $m^3.s^{-1}$) was measured through a digital flowmeter. The lateral surface of the cylindrical samples was sealed with aluminium foil tape and slightly confined with an inflated rubber tyre surrounding the sample, thus ensuring a uniaxial gas flow.

Assuming the validity of Darcy's law for a steady state unidirectional gas flow in a porous media, the apparent permeability at the tested temperature T° ($k_{appT°}$, m^2) was calculated from Eq. 1:

$$k_{app_{T°}} = \frac{2 \text{ x } \mu \text{ x } Q_v \text{ x } L_{T°} \text{ x } P_{atm}}{A_{T°} \text{ x } ({P_{inj}}^2 - {P_{atm}}^2)} \quad (1)$$

where: µ is the dynamic viscosity of the nitrogen gas (1.75 x 10^{-5} Pa.s at 20 °C), P_{atm} is the atmospheric pressure (101 325 Pa) while $L_{T°}$ and $A_{T°}$ are respectively the thickness (m) and the cross-sectional area (m^2) of the specimen at the tested temperature T°.

The residual intrinsic permeability (k_{int}) is determined from the linear regression of the apparent permeability values, at the different nitrogen pressures, as the threshold permeability between the viscous flow and slip flow [30], i.e. the value of apparent permeability at an infinite inverse mean pressure ($1/P_m$, with P_m being the mean pressure of injected pressure P_{inj} and atmospheric pressure P_{atm}).

3. Results and analysis

3.1 TG-DSC tests

Figure 2 and Figure 3 show results from the TG-DSC tests performed on SW50 and SWC3.5 samples, either equalised at 25 °C (control sample) or exposed to 350 °C. The mass loss curves during the temperature rise are detailed in Figure 2, and its derivative in Figure 3. Inspection of these figures indicates that the control sample SWC3.5 exhibited the largest mass loss (-0.72%) between 115 °C and 150 °C. This is due to the bonded-water loss from both the calcium-silicate-hydrate (C-S-H) and calcium-aluminate-hydrate (C-A-H) gels of cementitious phases, as also observed by Sharma et al. (2012) [31] and Baldusco et al. (2019) [32]. Instead, SW50 samples equalised at 25 °C exhibited a lower mass loss over the same temperature range, essentially due to the evaporation of weakly bonded adsorbed water.

As expected, both SW50 and SWC3.5 samples, preliminarily exposed to a temperature of 350 °C, respectively exhibited a comparable mass loss of 0.17% and 0.25% over the same temperature range 115–150 °C, which was lower than that measured on the same materials equalised at room temperature. This is because the preliminary exposure to 350 °C has induced partial dehydration of both the C-S-H and C-A-H gels in the case of SWC3.5 samples and evaporation of both adsorbed and bonded water in the case of SW50 samples. Results also indicate that all samples exhibited a main mass loss at temperatures comprised between 650 °C and 800 °C. The SW50 samples exhibiting the largest mass loss of 3.79% because of the hydroxylation of the illitic clay fraction of the material, as also experimentally observed by Gualtieri and Ferrari (2006) [33]. This aspect was less evident in the unstabilised earth previously exposed at 350 °C (mass loss was equal to 2.44%) as well as in comparison with

cement stabilised samples. This can be due to the presence of the cementing bonds that may have shielded the illitic clay fraction from the effect of temperature. Instead, the mass reduction measured on SWC3.5 samples over the same temperature range (between 650 °C and 800 °C) is rather attributed to the decomposition of calcium carbonate (CaCO3) in calcium oxide (CaO) and carbon dioxide (CO2), as also observed by Dash et al. (2022) [34]. This outcome was not affected by the preliminary temperature exposure as both SWC3.5 samples, either exposed to 350 °C or equalised at 25 °C, exhibited a very similar mass loss of 2.88% and 2.72%, respectively. This finding suggests that the preliminary exposure to 350 °C did not affect the strength of CaCO3 bonds, which only started to degrade at temperatures above 650 °C [34].

In summary, the SW50 and SWC3.5 samples equalised at 25 °C exhibited different decomposition kinetics as temperature increased because of the cement stabilisation. This difference is almost erased after exposure to 350 °C, with both SW50 and SWC3.5 samples showing very similar variations of mass loss and its derivative with temperature with only a fairly small difference between them in the 650-800 °C range.

The similar behavior of these two materials at high temperatures suggests that this type of test, at least in this case, was not effective in distinguishing significant differences in the microstructural response of the materials to heat (evidenced by similar mass loss variations). Consequently, inadequate conclusions could be drawn from this test to explain why SW50 exhibited thermal instability while SWC3.5 remained thermally stable, as observed in previous studies.

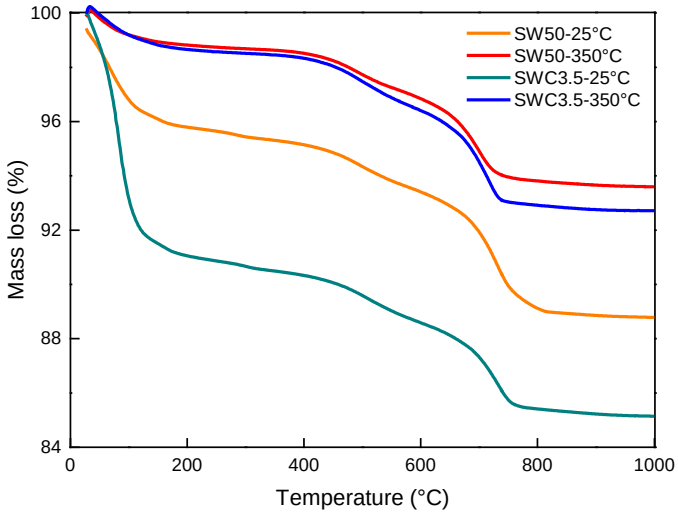

Figure 2. TG-DSC results - mass loss variation with temperature increase of SW50 and SWC3.5 samples, control (25°C) and exposed to 350°C

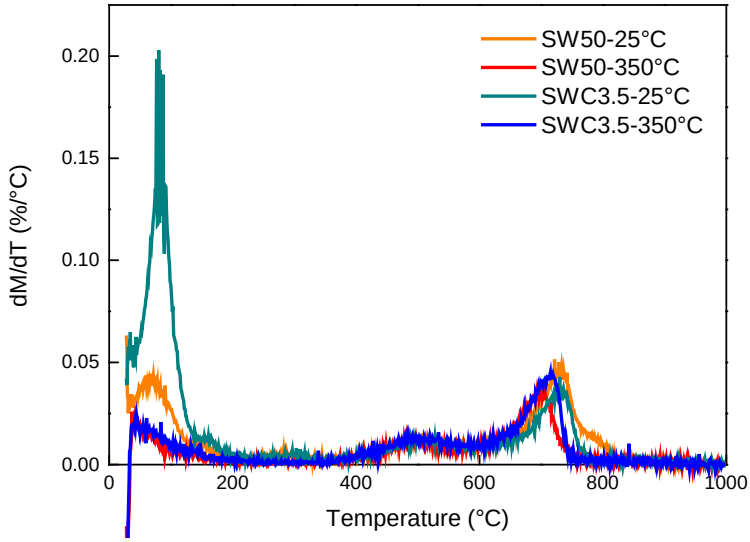

Figure 3. TG-DSC results – derivative of mass loss with temperature increase of SW50 and SWC3.5 samples, control (25°C) and exposed to 350°C

3.2 FTIR tests

Figure 4 shows results from FTIR tests performed on both SW50 and SWC3.5 samples either equalised at 25 °C or exposed to 350 °C. As see from Figure 4, SW50 samples equalised at 25 °C exhibited the largest reduction of transmittance at wavenumbers ranging from 400 cm^{-1} to 1200 cm^{-1} with minimum peaks at 420 cm^{-1} and 1000 cm^{-1}, which indicates the presence of strong Si–O–Si covalent bonds in the vitreous phase of the unstabilised silica-rich earthen material [28,35]. These Si–O–Si covalent bonds found in SW50 samples are weakened by both the cement stabilisation and the temperature exposure, as also found by Bruno et al. (2018) [36] and Bruno et al. (2019) [21]. Cement stabilisation has modified the Si–O–Si covalent bonds and the vitreous phase of the siliceous minerals to form a calcium-silicate-hydrate (C-S-H) gel, which has reduced the adsorption-desorption capacity of the material. This feature emerged from the adsorption-desorption tests (as described in the following section) and it was also experimentally observed by Bahmani et al. (2014) [37] on cement stabilised residual clayey soils. Figure 4 also shows that the exposure to 350 °C has reduced the transmittance at wavenumbers ranging from 400 cm^{-1} to 1200 cm^{-1} for both SW50 and, to a lower extent, SWC3.5 samples, which suggests that cement stabilisation has rendered the earth materials less sensitive to temperature exposure.

The observed lower transmittance of wavenumbers aligns with the findings of Abdallah et al. (2024) [11], who reported that cement-stabilized samples exhibited no signs of thermal instability. This stability is attributed to cement stabilization, which reduces the sensitivity of earthen materials to temperature exposure. While the FTIR results and the corresponding transmittance behavior offer valuable insights into potential microstructural changes under high temperatures, further in-depth analysis is necessary. Additional mineralogical-scale investigations are required to precisely understand these changes and establish a clearer link between the material's thermal behavior and the previously observed fire test results.

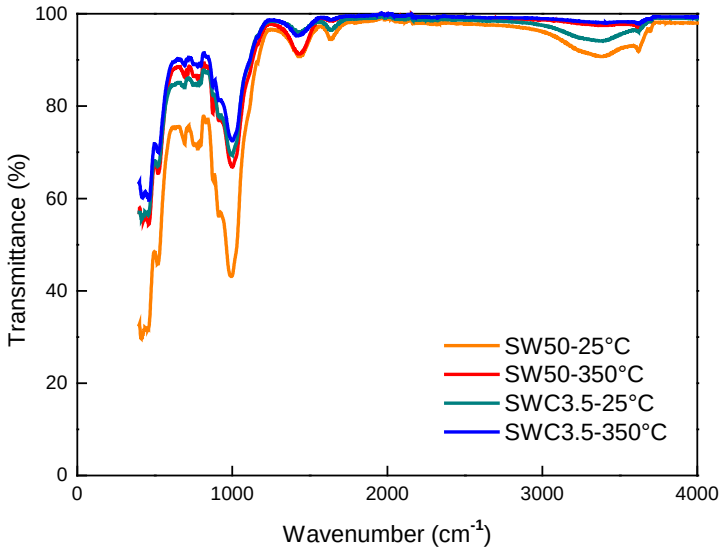

Figure 4. Results from FTIR tests on SW50 and SWC3.5 samples control (25°C) and exposed to 350°C

3.3 Isothermal sorption tests

Figure 5 shows the results from isothermal sorption-desorption tests performed on both SW50 and SW3.5 samples either equalised at 25 °C or exposed at 350 °C. In particular, Figure 5a and Figure 5b, respectively, present results in terms of percentage mass variation and corresponding hysteresis, with the latter being calculated as the difference between the percentage mass variations measured during desorption and sorption at the same relative humidity level.

SW50 samples equalised at 25 °C exhibited the highest adsorption/desorption capacity (Figure 5a) with the lowest hysteresis (Figure 5b), which is particularly evident at high relative humidities. These findings are in agreement with the adsorption-desorption curve obtained by Bruno et al. (2020) [9] on a similar earth material but compacted at a different dry density. The higher adsorption capacity of the SW50 samples exposed to room temperature, can reasonably be considered among the most relevant factors that trigger its thermal instability as the material is exposed to high temperatures. Previous findings by Abdallah et al. [11] demonstrated the pronounced sensitivity of SW50 to water content; a sensitivity that led to the degradation of its mechanical properties. This degradation significantly influenced the material's overall fire behavior, highlighting the critical role of water adsorption in its thermal performance.

The sorption-desorption capacity is slightly reduced with a more pronounced hysteretic behaviour as the earth is stabilised with the addition of 3.5% cement. This is because the formation of C-S-H and C-A-H gels may have

inhibited the moisture buffering capacity of the illitic clay fraction, as also detected from the FTIR test. Moreover, these findings agree with experimental results obtained by Bruno et al. (2020) [9] and McGregor et al. (2014) [38], who measured a lower moisture buffering capacity of cement stabilised earth bricks compared with that of the unstabilised material. A reduced capacity to adsorb water combined with the protective effect of the newly formed C-S-H and C-A-H gels could make the cement-stabilised earth less prone to thermal instabilities upon exposure to high temperatures. Figure 5a also shows that both SW50 and SWC3.5 earth samples exhibit a similar reduced moisture buffering capacity after being exposed to 350 °C, similar to the experimental findings of Mbumbia et al. (2000) [39], Karaman et al. (2006) [40] and Bruno et al. (2019) [21] on thermally treated compressed earth bricks. This outcome suggests that both unstabilised and stabilised earth samples are less prone to exhibit thermal instabilities upon firing when they are preliminarily exposed to a high temperature. The latter outcome is in good agreement with the fire test results of Abdallah et al. (2024) [11], who found that SW50 and SWC3.5 samples did not exhibit thermal instability when exposed to fire, if they were preliminarily oven dried. Hence there will be lower built-up pressure on the pores at deeper cold layers inside the materials and thus lower risk of thermal instability.

Finally, results suggest that the effect of the water content, adsorbed at low temperatures, can considerably affect the fire behaviour of both unstabilised and cement-stabilised materials, as previously proved by Abdallah et al. (2024) [11]. While isothermal sorption tests did not provide a definitive indication of thermal instability, they revealed the material's mineralogical response to water adsorption and its sensitivity (or lack thereof). This sensitivity has been shown to be a potential indicator of earthen materials' behavior under fire conditions.

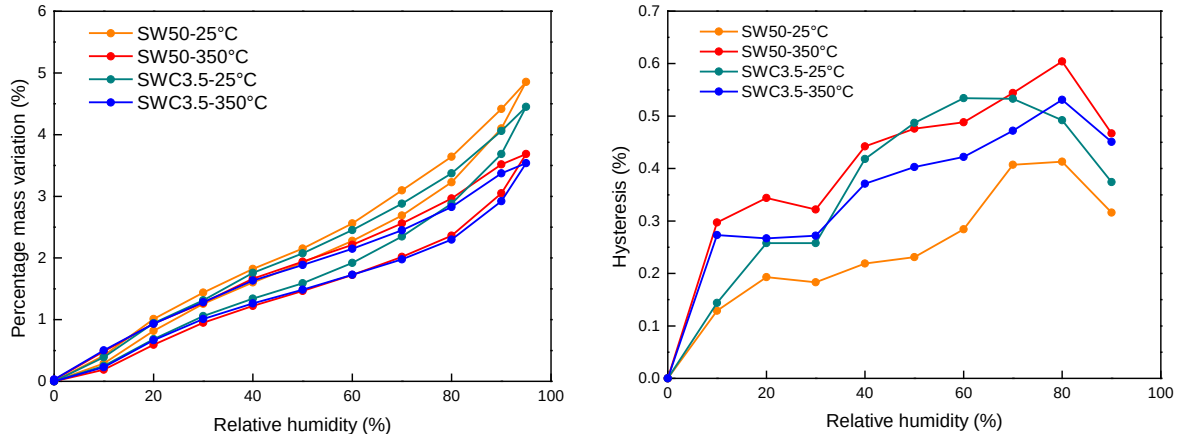

(a) (b)

Figure 5. Results from isothermal sorption/desorption tests, percentage mass variation (a) and hysteresis (b)

3.4 Residual gas permeability tests

The nitrogen gas permeability was measured on both SW50 and SWC3.5 samples exposed either to 80 °C (for drying) or to 350 °C. Figure 6 presents the variation of the residual intrinsic permeability with respect to the exposure temperature. SW50 samples exhibited a permeability which is one order of magnitude higher compared with that of SWC3.5 samples. The reduced permeability of cement stabilised samples is due to the formation of cement hydrates that fill porosity, totally or partially obstruct percolation pathways and bind soil particles together, thus limiting gas penetration within the material [41,42].

Figure 6 also shows that SW50 samples experienced a significant decrease in permeability between 80 °C and 350 °C, whereas SWC3.5 samples exhibited an almost constant permeability over the same temperature range. The reduced permeability of SW50 samples with temperature may be associated with the onset of a pyrolytic reaction and the decomposition of both calcium carbonate and organic matter that occur at temperatures of about 350 °C [43]. The drop was tough to explain because unstabilised materials do not suffer significant physicochemical changes at such high temperatures. Additional research is needed to better understand this result. However, it might have happened that it occurred as a result of some sort of decomposition of both carbonaceous and organic matters which could have generated gases with a relatively high internal pressure, which have occluded material pores and hindered the injection of pressure during permeability tests with the consequent decrease of material's permeability, as also observed in other experimental works [43]. Moreover, this decrease can correspond to a direct cause of a considerable increase of pore pressure during heating, especially at the inner and colder regions of the samples with a consequent decrease of the mechanical properties. This observation can confirm that unstabilised earth materials can start to exhibit thermal instabilities at a temperature of 350 °C, as suggested by previous results [11–13].

The lower permeability of SWC3.5 typically indicates a higher risk of thermal instabilities due to the condensation of water in inner material regions and consequent building up of higher pore vapour overpressures [44–46]. However, previous results showed an opposite trend with the SW50 sample exhibiting thermal instabilities while SWC3.5 being thermally stable [11]. In this regard, two counteracting observations can be made. On one hand, the higher permeability of SW50 samples, compared with the SWC3.5 ones, normally would indicate a looser fabric and a higher porosity, which generate lower vapour overpressures with water easily permeating the material during heating, as also observed in concrete exposed to fire [47–52]. On the other hand, instead, results from previous fire tests [11] show that large pore vapour overpressures were responsible for inducing thermal instabilities in SW50 samples and not in the SWC3.5 samples.

The above observations suggest that permeability measurements, while intrinsically dependent on the fabric of the material as well as not addressing the possible right range of porosity, do not seem fully representative of the microstructural changes occurring in an earthen sample exposed to high temperature.

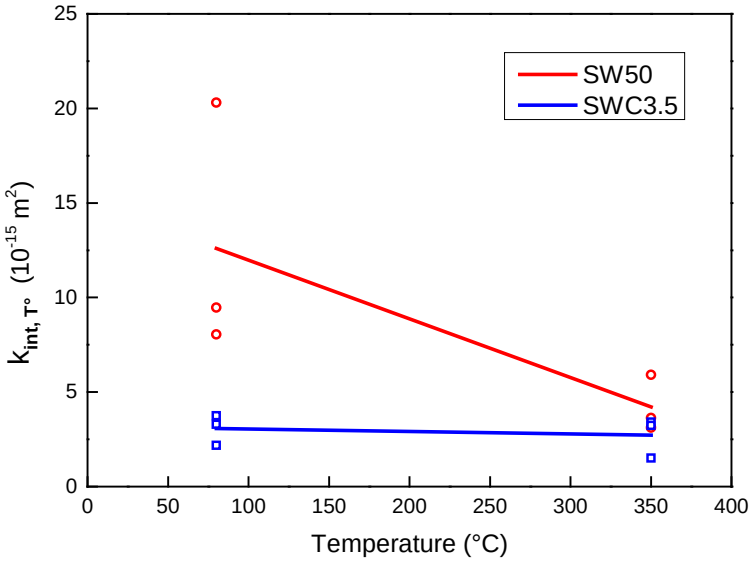

Figure 6. Intrinsic gas permeability of SW50 and SWC3.5 samples exposed to 80 and 350 °C

4. Conclusion and perspectives

This study investigated the effect of temperature on the mineralogy and adsorption-desorption behaviour of earthen materials. Outcomes from the present experimental campaign supported the interpretation of previously performed fire tests, especially concerning the role played by both mineralogical and hygroscopic properties on the onset of thermal instabilities as well as on the thermo-chemical changes of the materials caused by exposure to high temperatures. To this purpose, TG-DSC, FTIR, sorption-desorption and residual nitrogen gas permeability tests were performed on two types of earthen materials: unstabilised earthen samples compacted at 50 MPa (SW50) and cement stabilised samples compacted to the standard Proctor level (SWC3.5). These samples were firstly equalised at 25 °C and then heated to 350 °C.

The main outcomes from the present experimental campaign can be summarised as follows:

1) The SWC3.5 samples exhibited the largest mass reduction at temperatures below 200°C due to water loss from C-S-H and C-A-H gels, while the mass reduction between 650-800°C was attributed to dehydration of illitic clay fraction (SW50) and decomposition of calcium carbonate into calcium oxide and carbon dioxide (SWC3.5).

2) FTIR spectra showed that cement stabilisation has weakened Si-O-Si covalent bonds in favour of C-A-H and C-S-H formation, which is a key factor determining a better fire behaviour and high temperature resistance of SWC3.5 samples compared with SW50 ones.

3) The SW50 samples had the highest water adsorption capacity, making them more sensitive to thermal instabilities, while the SWC3.5 samples showed a lower adsorption capacity, reducing their tendency for instability.

4) Exposure to 350 °C significantly reduced the water adsorption capacity of both SW50 and SWC3.5 samples, thus minimising the risk of thermal instability due to successive increases in temperature.

5) SW50 had much higher permeability than SWC3.5, in contrast to prior testing in which behaviour was equivalent (at a temperature of 350 °C). This result questioned the concept that higher permeability indicates lower pore pressure and a looser fabric and structure, which was not the case in prior fire experiments that revealed the thermal instability of SW50 and the stability of SWC3.5, respectively.

6) Mineralogy may not accurately recognize instabilities during fire, thus permeability should be combined with further high-temperature tests to offer a more accurate indication.

The findings highlight the complexity of assessing the fire performance of earthen materials, emphasizing the need for more comprehensive and integrated testing approaches. Conventional high-temperature mineralogical analyses, hygroscopic thermal assessments and permeability measurements may not sufficiently capture the critical mineralogical and moisture-driven changes that influence thermal behavior. While cement stabilization proves effective in improving fire resistance by decreasing heat sensitivity, moisture content continues to play a pivotal role in determining thermal stability. Future research should explore advanced testing methods to better understand the thermo-hydro-mechanical interactions governing the fire response of earthen materials.

Subsequent research should be directed towards the investigation of the mineralogy of earthen materials over a wider temperature range compared to that investigated in the present work. Moreover, porosimetry tests (such as mercury intrusion and nitrogen adsorption tests) should also be performed to examine the changes in porosity for both materials at a deeper microstructural level. This will help clarify the effect of porosity on the build-up of pore vapour pressure that occurs inside heated samples during fire. Finally, residual thermal and mechanical tests should be performed to investigate the influence of the coupled thermo-hydro-mechanical behaviour of earth materials on the onset of thermal instabilities at high temperatures.

5. References

[1] Hall M, Allinson D. Assessing the effects of soil grading on the moisture content-dependent thermal conductivity of stabilised rammed earth materials. Appl Therm Eng. 2009;29(4):740-747.
[2] Ozel M. Determination of optimum insulation thickness based on cooling transmission load for building walls in a hot climate. Energy Convers Manag. 2013;66:106-114.
[3] Zhang L, Yang L, Jelle BP, Wang Y, Gustavsen A. Hygrothermal properties of compressed earthen bricks. Constr Build Mater. 2018;162:576-583.
[4] Hoffmann C, Alonso EE, Romero E. Hydro-mechanical behaviour of bentonite pellet mixtures. Phys Chem Earth Parts ABC. 2007;32(8-14):832-849.
[5] Tang AM, Cui YJ, Le TT. A study on the thermal conductivity of compacted bentonites. Appl Clay Sci. 2008;41(3-4):181-189.
[6] Bui QB, Morel JC, Venkatarama Reddy BV, Ghayad W. Durability of rammed earth walls exposed for 20 years to natural weathering. Build Environ. 2009;44(5):912-919.
[7] Bruno AW, Gallipoli D, Perlot C, Mendes J. Effect of very high compaction pressures on the physical and mechanical properties of earthen materials. E3S Web Conf. 2016;9:14004.
[8] El Fgaier F, Lafhaj Z, Chapiseau C, Antczak E. Effect of sorption capacity on thermo-mechanical properties of unfired clay bricks. J Build Eng. 2016;6:86-92.
[9] Bruno AW, Gallipoli D, Perlot C, Kallel H. Thermal performance of fired and unfired earth bricks walls. J Build Eng. 2020;28:101017.
[10] Ávila F, Puertas E, Gallego R. Characterization of the mechanical and physical properties of unstabilized rammed earth: A review. Constr Build Mater. 2021;270:121435.
[11] Abdallah R, Carré H, Perlot C, Borderie CL, Ghoche HE. Study of the risk of instability in earthen bricks subjected to fire. Mater Struct. 2024;57(1):16. https://link.springer.com/epdf/10.1617/s11527-023-02284-9
[12] Abdallah R, Carré H, McGregor F. Effect of compaction pressure on the risk of thermal instability of compressed earth bricks. Mater Struct. 2024;57(4):84.
[13] Abdallah R. The influence of thermal gradients on the fire behavior of raw earth and cement stabilized bricks at various water contents. Acad J Civ Eng. 2022;40.1.
[14] International standard. ISO 834-1. Fire resistance tests -- Elements of building construction. International Organization for Standardization; 1999.
[15] Johari I, Said S, Hisham B, Bakar A, Ahmad ZA. Effect of the change of firing temperature on microstructure and physical properties of clay bricks from Beruas (Malaysia). Sci Sinter. 2010;42(2):245-254.
[16] Rani J, Singh KJ, Singh R, Sublania H. Effect on Microstructure of Clay Bricks after Firing Temperature. J Emerg Technol Innov Res. 2015;2(10):6.
[17] Geng J, Sun Q. Effects of high temperature treatment on physical-thermal properties of clay. Thermochim Acta. 2018;666:148-155.
[18] Cultrone G, Sebastián E, Elert K, de la Torre MJ, Cazalla O, Rodriguez-Navarro C. Influence of mineralogy and firing temperature on the porosity of bricks. J Eur Ceram Soc. 2004;24(3):547-564.
[19] Amkpa JA, Badarulzaman NA, Aramjat AB. Influence of Sintering Temperatures on Physico-Mechanical Properties and Microstructure of Refractory Fireclay Bricks. Int J Eng Technol. 2017;8.
[20] Bruno AW. Hygro-mechanical characterisation of hypercompacted earth for building construction. [PhD Thesis]. Université de Pau et des Pays de l'Adour; 2016. [in France]

[21] Bruno AW, Gallipoli D, Perlot C, Mendes J. Optimization of bricks production by earth hypercompaction prior to firing. J Clean Prod. 2019;214:475-482.
[22] NF EN 197-1. Cement - Part 1: Composition, specifications and conformity criteria for common cements. 2012 (in French).
[23] Abdallah RI, Perlot C, Carré H, La Borderie C, EL Ghoche H. Fire Behavior of Raw Earth Bricks: Influence of Water Content and Cement Stabilization. Constr Technol Archit. 2022;1:792-800.
[24] Abdul Kadir A, Mohajerani A. Physical and Mechanical Properties of Fired Clay Bricks Incorporated with Cigarette Butts: Comparison between Slow and Fast Heating Rates. Appl Mech Mater. 2013;421:201-204.
[25] Farage MCR, Sercombe J, Gallé C. Rehydration and microstructure of cement paste after heating at temperatures up to 300 °C. Cem Concr Res. 2003;33(7):1047-1056.
[26] Akinshipe O, Kornelius G. Chemical and Thermodynamic Processes in Clay Brick Firing Technologies and Associated Atmospheric Emissions Metrics-A Review. J Pollut Eff Control. 2017;05(02).
[27] Serra MF, Conconi MS, Suarez G, Agietti EF, Rendtorff NM. Firing transformations of an argentinean calcareous commercial clay. Ceramica. 2013;59(350):254-261.
[28] Margenot AJ, Calderón FJ, Goyne KW, Mukome FND, Parikh SJ. IR Spectroscopy, Soil Analysis Applications. In: Lindon JC, Tranter GE, Koppenaal DW. Encyclopedia of Spectroscopy and Spectrometry (Third Edition) [Internet]. Oxford: Academic Press; 2017. p. 448-454. https://www.sciencedirect.com/science/article/pii/B9780124095472121705
[29] Kollek JJ. The determination of the permeability of concrete to oxygen by the Cembureau method - a recommendation. Mater Struct. 1989;22:6.
[30] Klinkenberg LJ. The permeability of porous media to liquids and gases. In: American Petrolium Institute, Drilling and Production Practice. American Petrolium Institute, Drilling and Production Practice; 1941. p. 200-213.
[31] Sharma NK, Swain SK, Sahoo UC. Stabilization of a Clayey Soil with Fly Ash and Lime: A Micro Level Investigation. Geotech Geol Eng. 2012;30(5):1197-1205.
[32] Baldusco R, Nobre TRS, Angulo SC, Quarcioni VA, Cincotto MA. Dehydration and Rehydration of Blast Furnace Slag Cement. J Mater Civ Eng. 2019;31(8):04019132.
[33] Ferrari S, Gualtieri AF. The use of illitic clays in the production of stoneware tile ceramics. Appl Clay Sci. 2006;32(1):73-81.
[34] Dash MK, Patro SK, Acharya PK, Dash M. Impact of elevated temperature on strength and micro-structural properties of concrete containing water-cooled ferrochrome slag as fine aggregate. Constr Build Mater. 2022;323:126542.
[35] Rios S, Cristelo N, Viana da Fonseca A, Ferreira C. Structural Performance of Alkali-Activated Soil Ash versus Soil Cement. J Mater Civ Eng. 2016;28(2):04015125.
[36] Bruno AW, Perlot C, Mendes J, Gallipoli D. A microstructural insight into the hygro-mechanical behaviour of a stabilised hypercompacted earth. Mater Struct Constr. 2018;51(1):17.
[37] Bahmani SH, Huat BBK, Asadi A, Farzadnia N. Stabilization of residual soil using SiO2 nanoparticles and cement. Constr Build Mater. 2014;64:350-359.
[38] McGregor F, Heath A, Shea A, Lawrence M. The moisture buffering capacity of unfired clay masonry. Build Environ. 2014;82:599-607.
[39] Mbumbia L, Mertens de Wilmars A, Tirlocq J. Performance characteristics of lateritic soil bricks fired at low temperatures: a case study of Cameroon. Constr Build Mater. 2000;14(3):121-131.
[40] Karaman S, Ersahin S, Gunal H. Firing temperature and firing time influence on mechanical and physical properties of clay bricks. J Sci Ind Res. 2006;65:7.
[41] Rahman ZA, Sulaiman N, Rahim SA, Idris WMR, Lihan T. Effect of cement additive and curing period on some engineering properties of treated peat soil. Sains Malays. 2016;45(11):1679-1687.
[42] Diana W, Hartono E, Muntohar AS. The Permeability of Portland Cement-Stabilized Clay Shale. IOP Conf Ser Mater Sci Eng. 2019;650:012027.
[43] Meng T, Liu R, Meng X, Zhang D, Hu Y. Evolution of the permeability and pore structure of transversely isotropic calcareous sediments subjected to triaxial pressure and high temperature. Eng Geol. 2019;253:27-35.
[44] T. Z. H. Effect of moisture on the fire endurance of building elements. In: Moisture in materials in relation to fire tests ASTM International. 1965;74-95.
[45] Mindeguia JC, Carré H, Pimienta P, La Borderie C. Experimental discussion on the mechanisms behind the fire spalling of concrete: Mechanisms Behind The Fire Spalling Of Concrete. Fire Mater. 2015;39(7):619-635.
[46] Liu JC, Tan KH, Yao Y. A new perspective on nature of fire-induced spalling in concrete. Constr Build Mater. 2018;184:581-90.

[47] McNamee R, Boström L. The Influence of Pressure in the Pore System on Fire Spalling of Concrete. Fire Technol. 2009;46:217-230.
[48] McNamee R. Fire spalling theories-Realistic and more exotic ones. In: Proceedings of the 6th International RILEM Workshop on Concrete Spalling. Sheffield, UK; 2019.
[49] Khoury GA, Anderberg Y. Concrete spalling review. Fire Saf Des. 2000;60:5-12.
[50] Mindeguia JC, Pimienta P, Noumowé A, Kanema M. Temperature, pore pressure and mass variation of concrete subjected to high temperature — Experimental and numerical discussion on spalling risk. Cem Concr Res. 2010;40(3):477-487.
[51] Zeiml M, Leithner D, Lackner R, Mang HA. How do polypropylene fibers improve the spalling behavior of in-situ concrete? Cem Concr Res. 2006;36(5):929-942.
[52] Gabriel Alexander Khoury. Effect of fire on concrete and concrete structures. Prog Struct Eng Mater. 2000;2.4:429-447.